J. Fluid Mech. (1990), *vol.* 211, *pp.* 157–182
Printed in Great Britain

A visual study of the flow around an oscillating circular cylinder at low Keulegan–Carpenter numbers and low Stokes numbers

By M. TATSUNO[1] AND P. W. BEARMAN[2]

[1] Research Institute for Applied Mechanics, Kyushu University, Kasuga 816, Japan
[2] Department of Aeronautics, Imperial College, London, SW7 2BY, UK

(Received 4 January 1989 and in revised form 18 July 1989)

The structures of the flow induced by a circular cylinder performing sinusoidal oscillations in a fluid at rest are investigated by means of flow visualization. The experiments are carried out at Keulegan–Carpenter numbers between 1.6 and 15 and at Stokes numbers between 5 and 160. Above a certain value of Keulegan–Carpenter number, depending on the Stokes number, some asymmetry appears in the flow separation and the associated vortex development behind the cylinder. The two vortices that are developed in a half cycle differ in strength and may be convected in different directions. This results in a fascinating set of flow patterns. Eight different regimes of flow can be identified within the ranges of Keulegan–Carpenter number and Stokes number studied. Furthermore, most of the resulting flows show a three-dimensional instability along the axis of the cylinder. Measurements of the wavelength of these disturbances are presented.

1. Introduction

It is well known that when a bluff body is oscillated in a still fluid or a fixed body is placed in an oscillating flow, secondary streaming is generated around the body owing to the influence of nonlinear effects (see for example Andrade 1931; Schlichting 1932; Tatsuno 1973, 1981). On the other hand, when the amplitude of oscillation of a body or a flow is increased beyond a certain critical value, flow separation occurs on the body surface and vortices are formed in each half cycle (see Bearman *et al.* 1981). Here separation is defined as a breaking away of the boundary layer from the body surface.

When the relative flow past a cylinder is undergoing sinusoidal oscillations the structure of the flow generated by the cylinder depends mainly on two parameters. These are the Keulegan–Carpenter number, KC, where $KC = 2\pi a/d$ and a is the amplitude of the relative motion and d is the cylinder diameter and the Stokes number, fd^2/ν, where f is the frequency of flow oscillation and ν the kinematic viscosity of the fluid. We will follow the nomenclature of Sarpkaya (1986) and give this latter number the symbol β. Many authors have presented measurements of the forces acting on a circular cylinder in oscillatory flow as a function of KC and β; results at large β have application to the prediction of the loading on ocean structures exposed to waves. There is also considerable fundamental interest in these flows and in the ways in which vortices are generated and shed.

Williamson (1985) investigated the relation between the motions of vortices and the forces exerted on a circular cylinder for cylinder amplitudes giving KC values up

to 60. He carried out experiments in a tank of water with a vertical cylinder and observed the motions of vortices on the surface of the water. Several vortex-shedding patterns were found and each pattern was observed to occur within a certain KC range. He did not examine, however, the three-dimensional structure of the flow along the cylinder axis. Honji (1981) has shown that a three-dimensional instability of the flow occurs around a circular cylinder oscillating in a fluid at rest. He carried out flow-visualization experiments for $68.8 < \beta < 700$, and observed that, in a certain range of KC, an instability of the flow developed that resulted in the appearance of streaks which arrange alternately in a double row along the cylinder axis.

The purpose of the present study is to investigate in detail the structure of the flows induced by a circular cylinder performing sinusoidal oscillations in a fluid at rest for $KC < 15$ and for $\beta < 160$. A number of different flow regimes have been observed involving separation and the generation of vortices. Many of these regimes have a spatially periodic pattern. The structure of each flow and the ranges of KC and β corresponding to each flow regime have been examined by means of flow-visualization techniques.

2. Apparatus and experimental methods

Experiments were performed using a tank filled with water, in which a vertical circular cylinder was oscillated sinusoidally. Two kinds of apparatus were used in this study. The apparatus which was used in a laboratory of the Research Institute for Applied Mechanics is shown schematically in figure 1. The tank has internal dimensions of 70 cm long and 38 cm deep by 40 cm wide, and two circular cylinders were used with diameters of 1.0 cm and 1.5 cm. The cylinder was attached at its upper end to a slider, which was oscillated along a rail by means of a scotch yoke mechanism. The other apparatus, which was used in a laboratory of Imperial College, consisted of a tank with internal dimensions of 2 m long, 50 cm deep and 61 cm wide and an oscillating carriage driven by a servo-controlled motor. A vertical cylinder of 2.0 cm diameter was used in this apparatus. In both the facilities, the gap between the bottom tip of the cylinders and the tank was smaller than 0.3 cm. As the cylinder motions were very slow, little or no surface waves were generated. Similar results were obtained in the two facilities.

Two methods were used for flow visualization. One was the electrolytic precipitation method (e.p. method), which was described in Taneda, Honji & Tatsuno (1979) and Honji, Taneda & Tatsuno (1980). A white dye of metallic compound was produced electrochemically from the surface of a cylinder. The other technique used was the aluminium dust method (A1 method), in which aluminium flakes ranging up to about 10 μm in length were suspended uniformly in the water. Several cross-sectional planes around the cylinder were illuminated through slits and the flow pattern in each plane was photographed using a camera fixed with respect to the undisturbed fluid.

The coordinate system used is shown in figure 2. The Z-axis is taken along the axis of the cylinder, in its mean position, and the cylinder oscillates along the X-axis. The Y-axis is at right angles to both the X- and Z-axes. The horizontal plane perpendicular to the cylinder axis is the (X, Y)-plane, the vertical plane parallel to the oscillation direction is the (X, Z)-plane and the vertical plane perpendicular to the oscillation direction is the (Y, Z)-plane. In order to lessen the possible influence

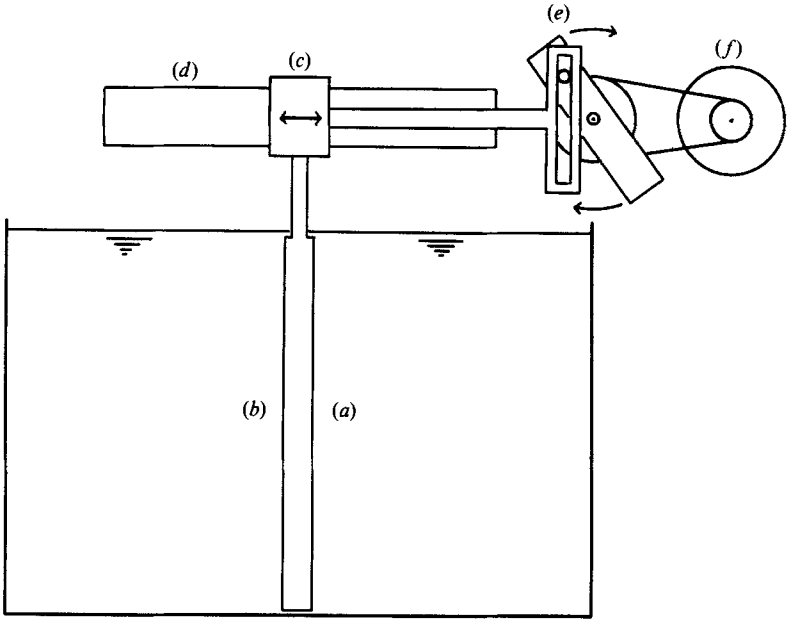

FIGURE 1. Schematic diagram of the experimental apparatus at the Research Institute for Applied Mechanics. Double arrow indicates the direction of cylinder oscillation. (*a*) Circular cylinder, (*b*) water tank, (*c*) slider, (*d*) fixed rail, (*e*) scotch yoke, (*f*) motor.

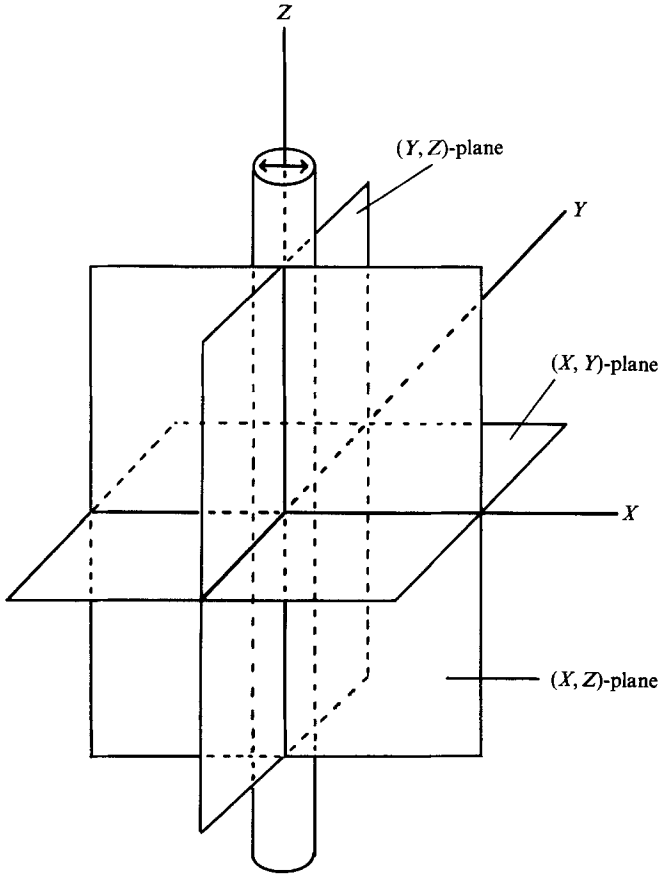

FIGURE 2. Coordinate system. Double arrow indicates the direction of cylinder oscillation.

of disturbances, a fresh experiment was started only after any motion of the water in the tank had subsided to a minimum level. Roughly 30 min were needed between runs.

3. Results

A number of different types of flow are found to appear for $KC < 15$ and $\beta < 160$, and they may be classified into several regimes according to their structure. The KC and β values for all the runs analysed are plotted in figure 3. Eight regimes were found and these are labelled A*–G. The structure of the flow in each regime will be explained in the following.

In photographs and drawings in this section a double arrow indicates the direction of oscillatory motion of the cylinder and a single arrow the direction of the cylinder travel or the direction of the flow. For each photograph of a flow pattern the values of a, d, f, KC and β are given together with the exposure time, t_e, used to take the picture.

3.1. *Regime* A*

Figure 4 shows a cross-sectional view of flow in regime A*. It is clear that no vortex shedding occurs. The flow in this regime, which for each β value is the regime occurring for the lowest KC numbers, is symmetrical with respect to the (X, Z)-plane and two-dimensional along the cylinder axis. An induced flow proceeds along the $(X, Z)-$plane away from the cylinder and flow approaches the cylinder along the (Y, Z)-plane in accordance with the law of conservation of mass. In figure 4, large regions of contra-rotating flow can be seen on both the far left- and far right-hand sides of the picture. These extend in the direction of oscillation and show a rolling up from the leading edges of the dye sheets.

3.2. *Regime* A

At values of KC larger than that of regime A* for $\beta < 50$, vortices are formed and the flow is composed of secondary streaming and flows due to vortices resulting from separation. The flow in regime A is symmetrical with respect to the (X, Z)-plane. Bearman *et al* (1981) have reported that vortex shedding will be initiated above some critical value of KC, which depends on the magnitude of β. However, as it is very difficult to determine the onset of vortex shedding, the critical value of KC distinguishing between the flow in regime A* and that in regime A is not shown in figure 3.

The process of vortex shedding following separation and vortex formation is illustrated in figure 5. In the figure, the arrow at the bottom of each photograph indicates the direction and length of cylinder travel during the exposure time. It is clear that two vortices, with rotations of opposite signs, are formed symmetrically behind the cylinder in each half cycle (figure 5*a*). At the end of a half cycle the two vortices stay behind the cylinder and as the cylinder reverses the vortices are convected towards the cylinder (figure 5*b*). However, these vortices do not survive into the next half cycle and may be cancelled by mixing with vorticity of opposite sign in the cylinder boundary layer (figure 5*c*), as has been suggested by Bearman *et al.* (1981).

Figure 6 shows patterns for the flow in the same regime visualized by means of the e.p. method. The white dye is shed from the cylinder simultaneously with a vortex. Concentrations of dye form two rows and drift with the induced flow. It should be noted that away from the cylinder the concentrations of dye do not represent

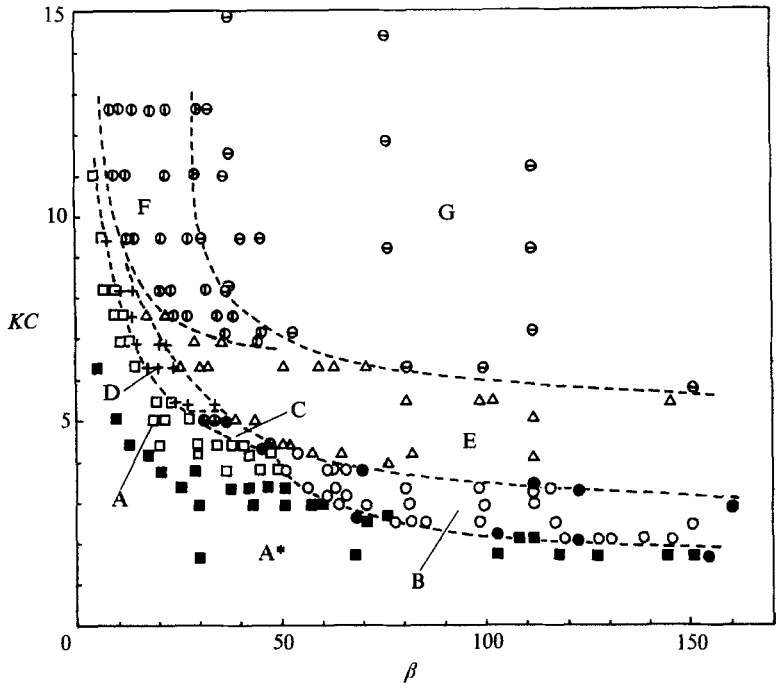

FIGURE 3. A classification of flows. Flow patterns are identified within eight regimes indicated A*–G. ■, A*; □, A; ○, B; ⊕, C; +, D; △, E; ⊙, F; ⊖, G; ●, critical values for appearance of a streaked flow by Honji (1981).

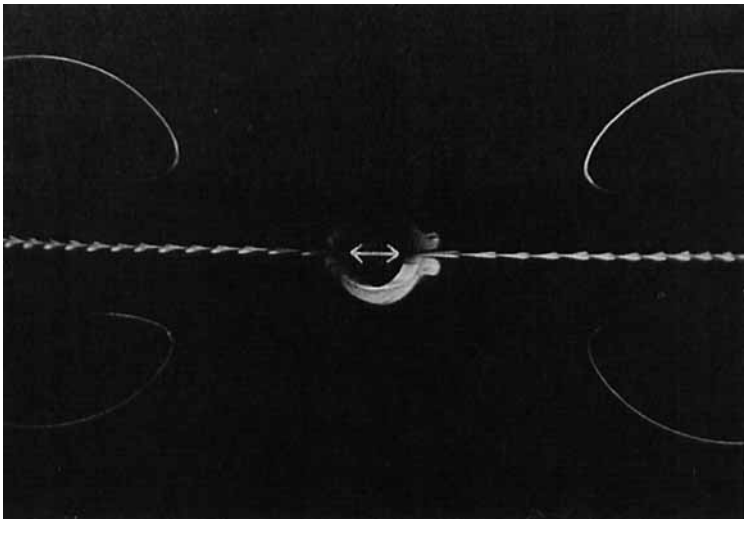

FIGURE 4. Plane view of flow in the (X, Y)-plane in regime A*. No vortex shedding occurs. E.p. method, $d = 1.0$ cm, $a = 0.50$ cm, $f = 0.755$ Hz, $KC = 3.14$, $\beta = 52.8$, $t_e = \frac{1}{8}$ s.

vortices, but mark periodic mass convection from the boundary layer on the cylinder. This finding is in contrast to that of Williamson who has shown that at larger β values symmetric vortex pairs are formed at flow reversal and two vortex pairs are shed from the cylinder in each half cycle.

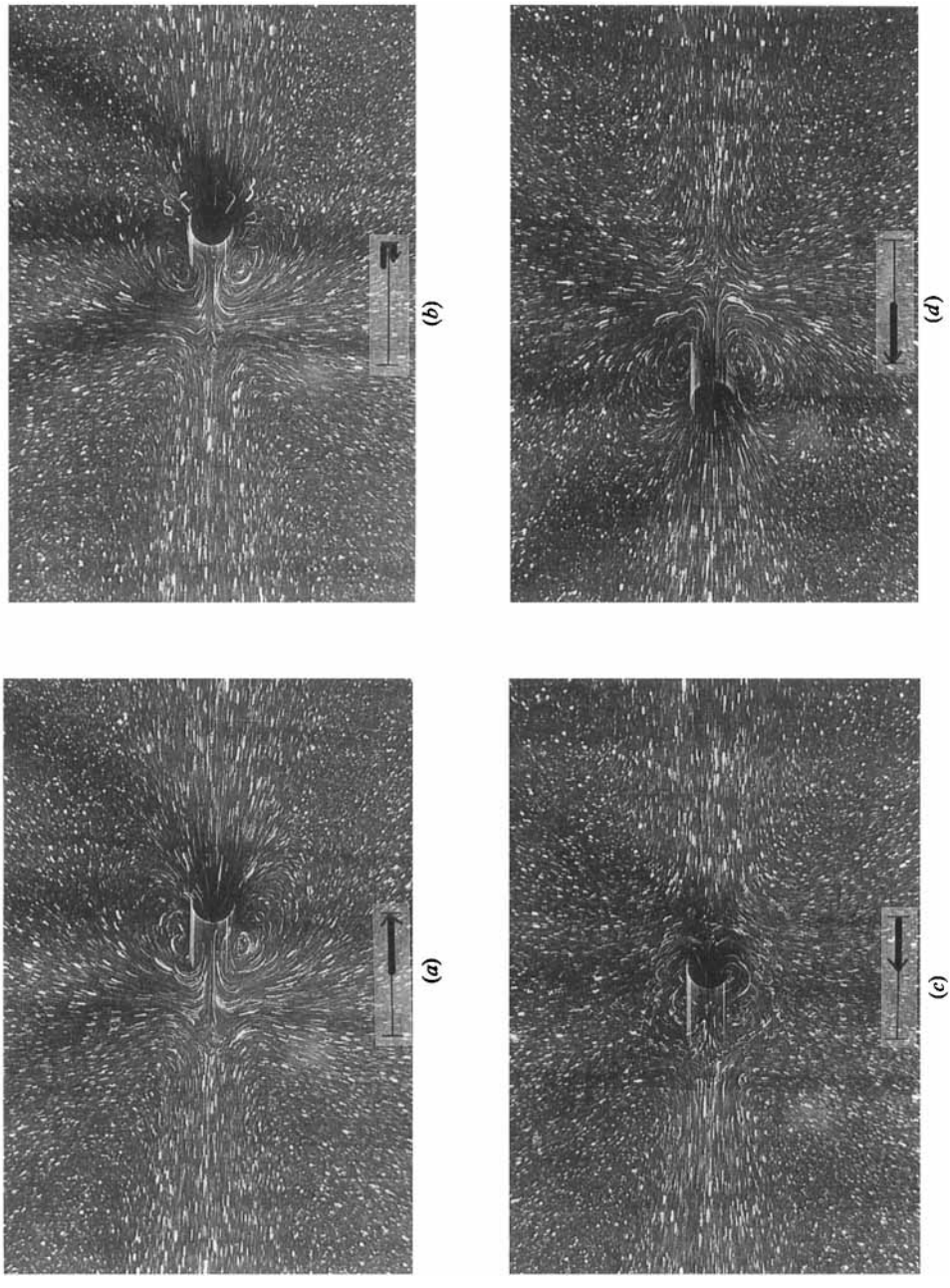

FIGURE 5. Plane view of flow in the (X, Y)-plane in regime A: A1 method, $d = 1.0$ cm, $a = 1.3$ cm, $f = 0.117$ Hz, $KC = 8.16$, $\beta = 8.18$, $t_e = 2$ s.

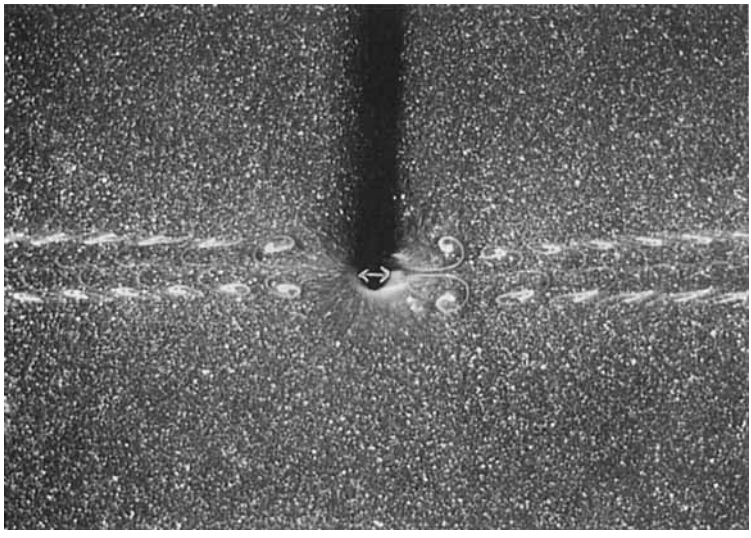

FIGURE 6. Plane view of flow in the (X, Y)-plane in regime A: e.p. method, $d = 1.0$ cm, $a = 1.75$ cm, $f = 0.097$ Hz, $KC = 11.0$, $\beta = 7.40$, $te = \frac{1}{4}$ s.

Figure 7 shows a view of the flow in the vertical (X, Z)-plane. It is clear, from the dye patterns running parallel to the cylinder, that the flow is two-dimensional.

3.3. *Regime* B

Figures 8–11 show different cross-sectional views of flows in regime B. The structure of this flow differs remarkably from that of other regimes. Vortices are not formed owing to flow separation, but a three-dimensional structure due to an instability in the boundary-layer flow appears near the cylinder surface. Figure 8 shows two views of the flow pattern in the (X, Y)-plane, where the lighter flow differs in spanwise position from that of the more intensely white flow.

Vertical views of the flow structure in the (X, Z)-plane and that in a plane parallel to the (X, Z)-plane are shown in figure 9 and figures 10 and 11, respectively. Honji (1981) investigated this flow in detail and named it 'the streaked flow'. The filled circles in figure 3 show the values of β and KC for which Honji observed 'the streaked flow'. From figures 8–11 and with reference to the work of Honji, it may be concluded that in regime B pairs of contra-rotating longitudinal vortices are formed alternately along the cylinder axis and extend in the direction of cylinder oscillation.

The distance (λ) between the centres of two 'streaked flows' adjacent to each other on one side of the cylinder was measured. In figure 12, average values of several measurements of λ/d are plotted against β for a number of values of KC and it can be seen that λ/d increases with KC. This tendency is similar to that found by Honji in the range $200 < \beta < 400$.

3.4. *Regime* C

Figure 13 shows a cross-sectional view of flow in regime C, observed by means of the e.p. method. Initially the dye sheets shed from the cylinder are aligned with the direction of oscillation but after several cycles they roll up to form large vortices. Large vortices of opposite sign are formed in succession for equal numbers of oscillation cycles. The large vortices are shown in figure 14, visualized by the A1 method. The arrangement of these vortices is similar to that in a Kármán vortex

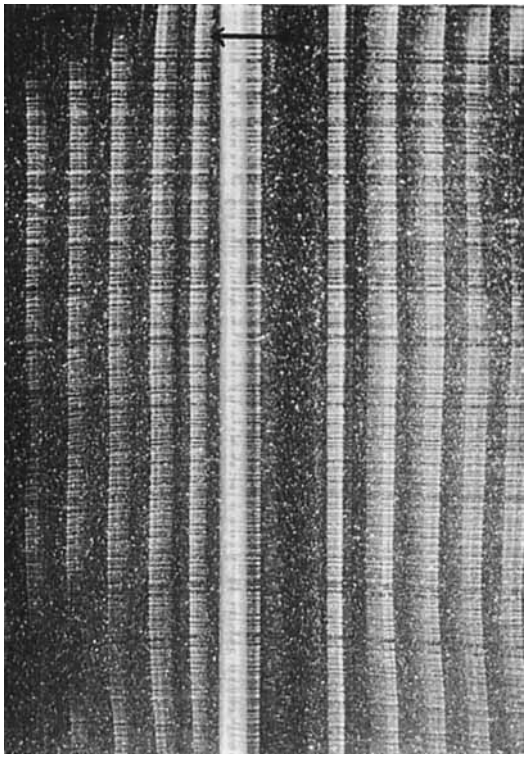

FIGURE 7. Plane view of flow in the (X, Z)-plane in regime A: e.p. method, $d = 1.0$ cm, $a = 1.75$ cm, $f = 0.097$ Hz, $KC = 11.0$, $\beta = 7.40$, $t_e = \frac{1}{4}$ s.

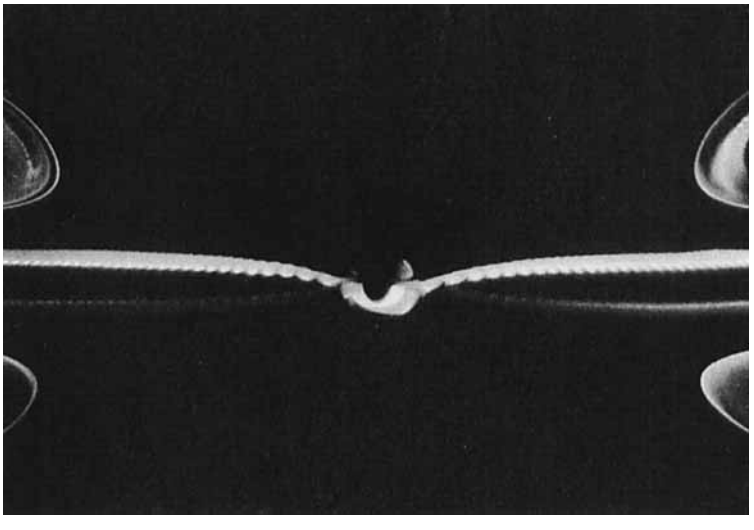

FIGURE 8. Plane view of flow in the (X, Y)-plane in regime B: e.p. method, $d = 1.0$ cm, $a = 0.50$ cm, $f = 0.88$ Hz, $KC = 3.14$, $\beta = 61.5$, $t_e = \frac{1}{8}$ s.

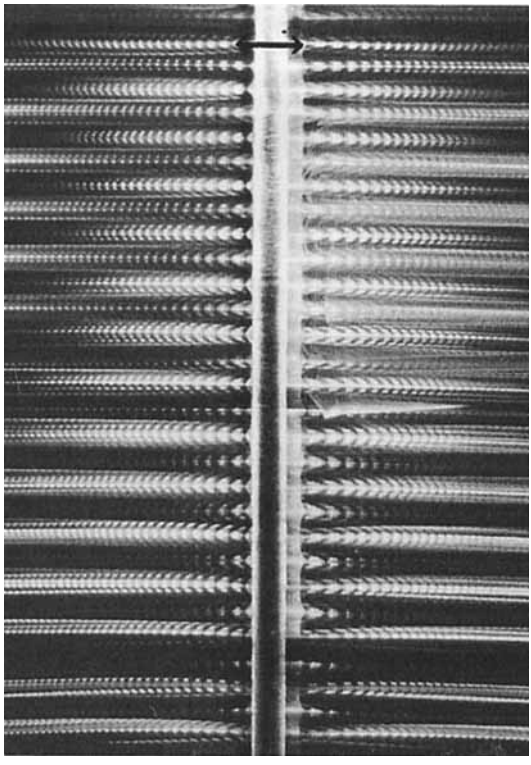

FIGURE 9. Plane view of flow in the (X, Z)-plane in regime B: e.p. method, $d = 1.0$ cm, $a = 0.50$ cm, $f = 0.88$ Hz, $KC = 3.14$, $\beta = 61.5$, $t_e = \frac{1}{15}$ s.

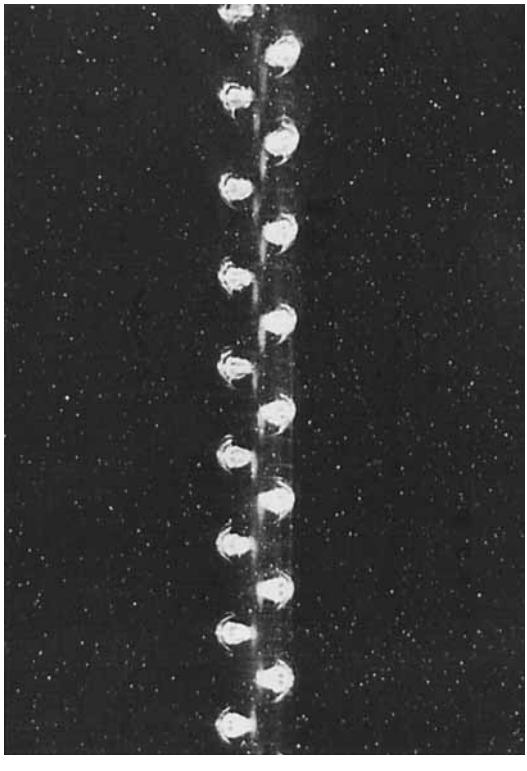

FIGURE 10. Plane view of flow in a plane at $X \doteqdot 2.5$ cm parallel to the (Y, Z)-plane in regime B: e.p. method, $d = 1.5$ cm, $a = 0.70$ cm, $f = 0.310$ Hz, $KC = 2.93$, $\beta = 77.7$, $t_e = \frac{1}{8}$ s.

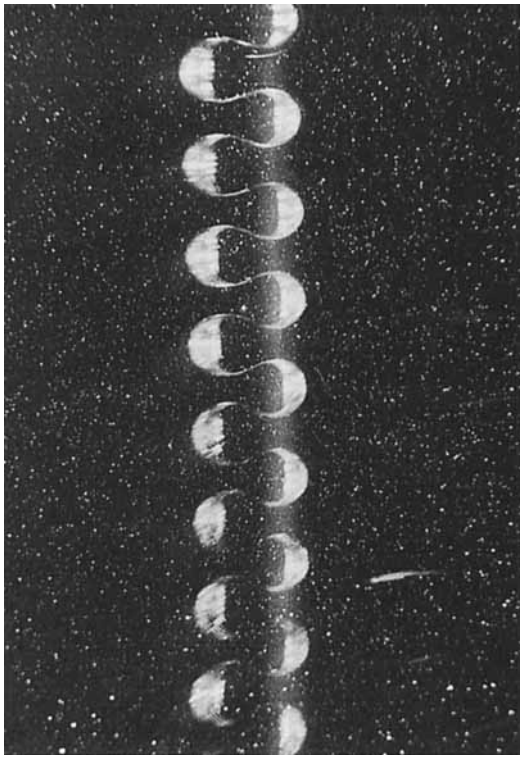

FIGURE 11. Plane view of flow in a plane at $X \doteqdot 5$ cm parallel to the (Y, Z)-plane in regime B: e.p. method, $d = 1.0$ cm, $a = 0.50$ cm, $f = 0.648$ Hz, $KC = 3.14$, $\beta = 72.6$, $t_e = \frac{1}{2}$ s.

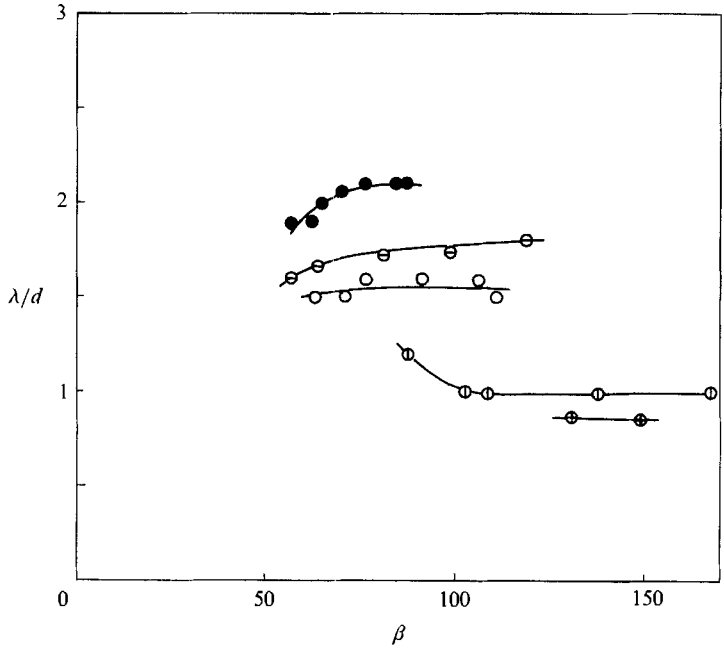

FIGURE 12. Distance between two streaked flows along one side of a cylinder in regime B. ●, $KC = 3.77$; ⊖, 3.35; ○, 3.14; ⓘ 2.51; ⊕, 2.09.

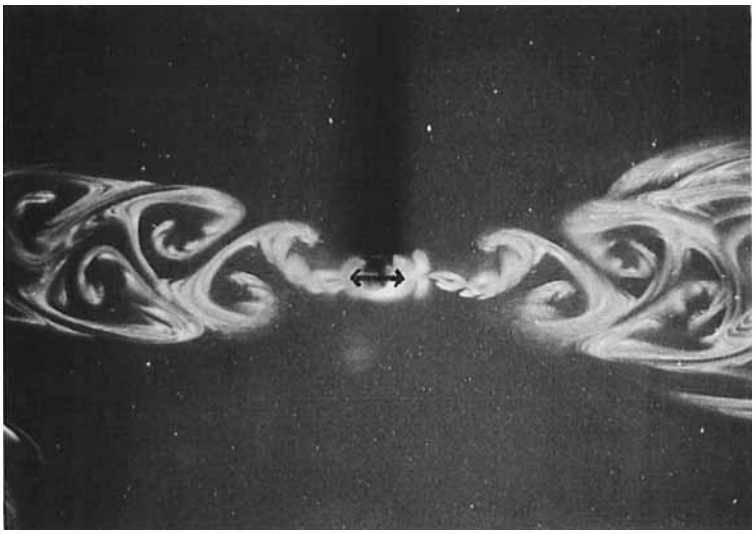

FIGURE 13. Plane view of flow in the (X, Y)-plane in regime C: e.p. method, $d = 1.0$ cm, $a = 0.70$ cm, $f = 0.646$ Hz, $KC = 4.40$, $\beta = 44.2$, $t_e = \frac{1}{2}$ s.

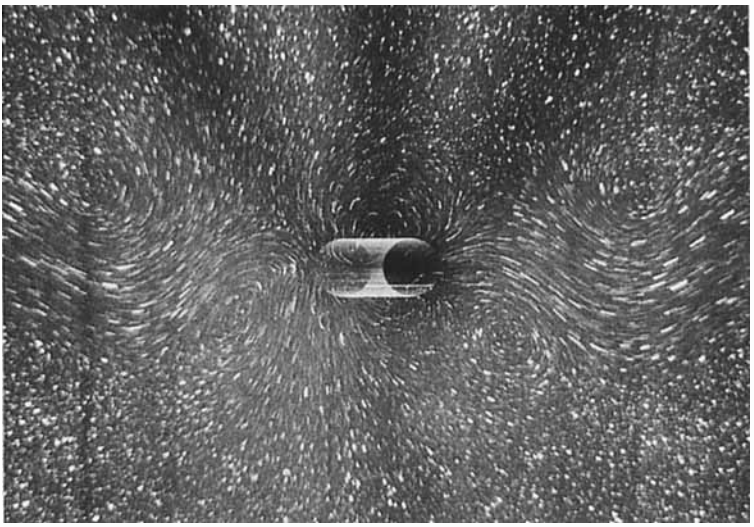

FIGURE 14. Plane view of flow in the (X, Y)-plane in regime C: A1 method, $d = 1.0$ cm, $a = 0.70$ cm, $f = 0.627$ Hz, $KC = 4.40$, $\beta = 47.9$, $t_e = \frac{1}{2}$ s.

street behind a cylinder in uniform flow. However the sense of rotation of the vortices is opposite to that found in a unidirectional flow wake and the vortices convect themselves away from the generating cylinder.

Figure 15 shows a dye pattern in the (X, Z)-plane and the flow is seen, in places, to be inclined to the cylinder. A cross-section through the wake in the (X, Z)-plane at $X \doteqdot 4.5$ cm is shown visualized by the e.p. method in figure 16. This again illustrates that the large vortices in this regime are inclined to the cylinder axis.

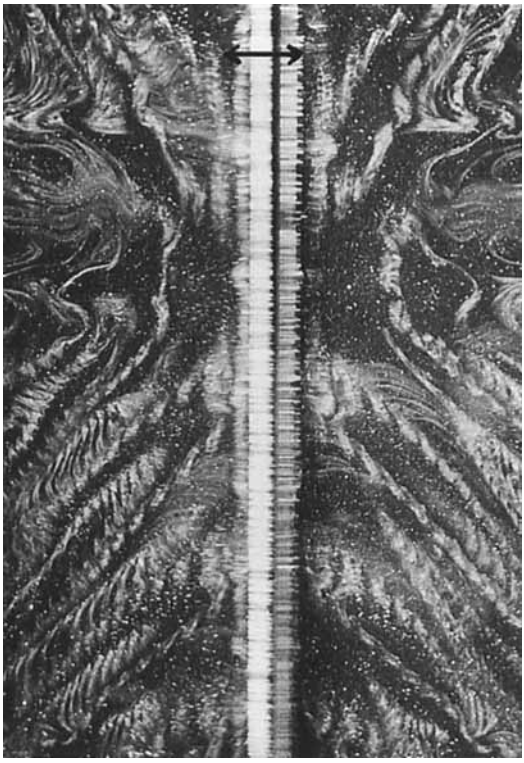

FIGURE 15. Plane view of flow in the (X, Z)-plane in regime C: e.p. method, $d = 1.0$ cm, $a = 0.70$ cm, $f = 0.440$ Hz, $KC = 4.40$, $\beta = 50.1$, $t_e = \frac{1}{4}$ s.

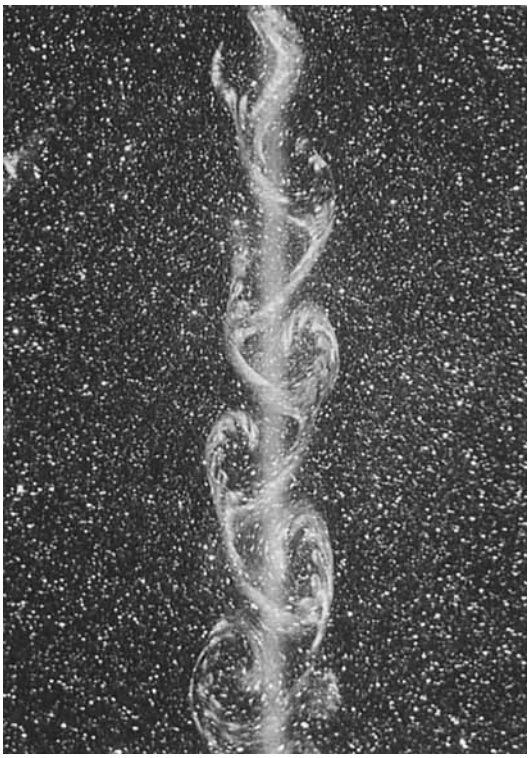

FIGURE 16. Plane view of flow in a plane at $X \doteqdot 4.5$ cm parallel to the (Y, Z)-plane in regime C: e.p. method, $d = 1.0$ cm, $a = 0.70$ cm, $f = 0.619$ Hz, $KC = 4.40$, $\beta = 46.9$, $t_e = 1$ s.

3.5. *Regime* D

In regimes A*, A, B and C, flow induced by the cylinder convects along the direction of cylinder oscillation. As the amplitude is increased, however, some asymmetry appears in the vortex development and induced flows deviate from the direction of oscillation.

Figure 17 shows flow patterns in the (X, Z)-plane at various stages of the motion in regime D. The arrow at the bottom of each photograph indicates the cylinder travel during the exposure time. When the cylinder translates from right to left, asymmetrical vortices, with opposite senses of rotation, are formed on the top and bottom sides of the cylinder (figure 17*a*), and the counterclockwise vortex on the lower side of the cylinder appears to grow stronger (figure 17*b*). As the cylinder reverses, the stronger vortex is convected back along the cylinder surface and shed obliquely across the axis of oscillation. Hence, the direction of the flow induced by the cylinder oscillation deviates from the direction of oscillation (figure 17*c*). In the half cycle from left to right, a clockwise vortex is developed on the lower side of the cylinder (figure 17*d*). In consequence, a strong vortex is developed on only one side of the axis of oscillation in each half cycle and the fluid mass accompanying the vortex is convected obliquely to the other side of the axis of oscillation. The overall flow pattern is symmetrical with respect to the Y-axis.

Figures 18 and 19 show flow patterns visualized by means of the e.p. method in the (X, Y)-plane. The deviation of the flow from the axis of oscillation is quite striking and the trails of the flow become more curved as the value of β is increased. It should be noted that the periodic dye patterns in the (X, Y)-plane, shown in figures 18 and 19, do not represent vortices, except near the cylinder.

The vertical dye pattern in the (X, Z)-plane is shown in figure 20 illuminated across a broad cross-section of the flow. It shows the flow has a three-dimensional structure in regime D and slightly faster moving fluid appears at certain intervals along the axis of the cylinder. Figure 21 shows a vertical view of the flow visualized by means of aluminium particles in a plane perpendicular to the trail of the curved flow. Aluminium particles glitter in groups at certain intervals along the axis of the cylinder. The regions where particles glitter in figure 21 correspond to regions where the flow is fast in figure 20. Rotating motion of the flow in these regions cannot be detected from the flow pattern in figure 21, which is different in character from the patterns in figures 10 and 11 in regime B and from the patterns in figures 28 and 29 in regime F (to be discussed later).

In conclusion, in regime D, tubes seem to be formed perpendicular to the cylinder at certain intervals along the axis of the cylinder, in which fluid is travelling faster than the surrounding fluid. The fluid flow in each tube does not form a longitudinal vortex.

The distance (λ) between the centres of two flow tubes adjacent to each other was measured and average values of several measurements of λ/d are plotted against β in figure 22. The values of λ/d seem to be independent of KC. The value of λ/d slightly decreases with increase of β.

3.6. *Regime* E

Figure 23 shows typical examples of the behaviour of the flow in regime E, where the flow changes with time. The photographs in figure 23 were taken in sequence during one run. The flow pattern in this regime temporarily resembles that in regime D. The flow which convects to one side of the axis of oscillation, however, intermittently

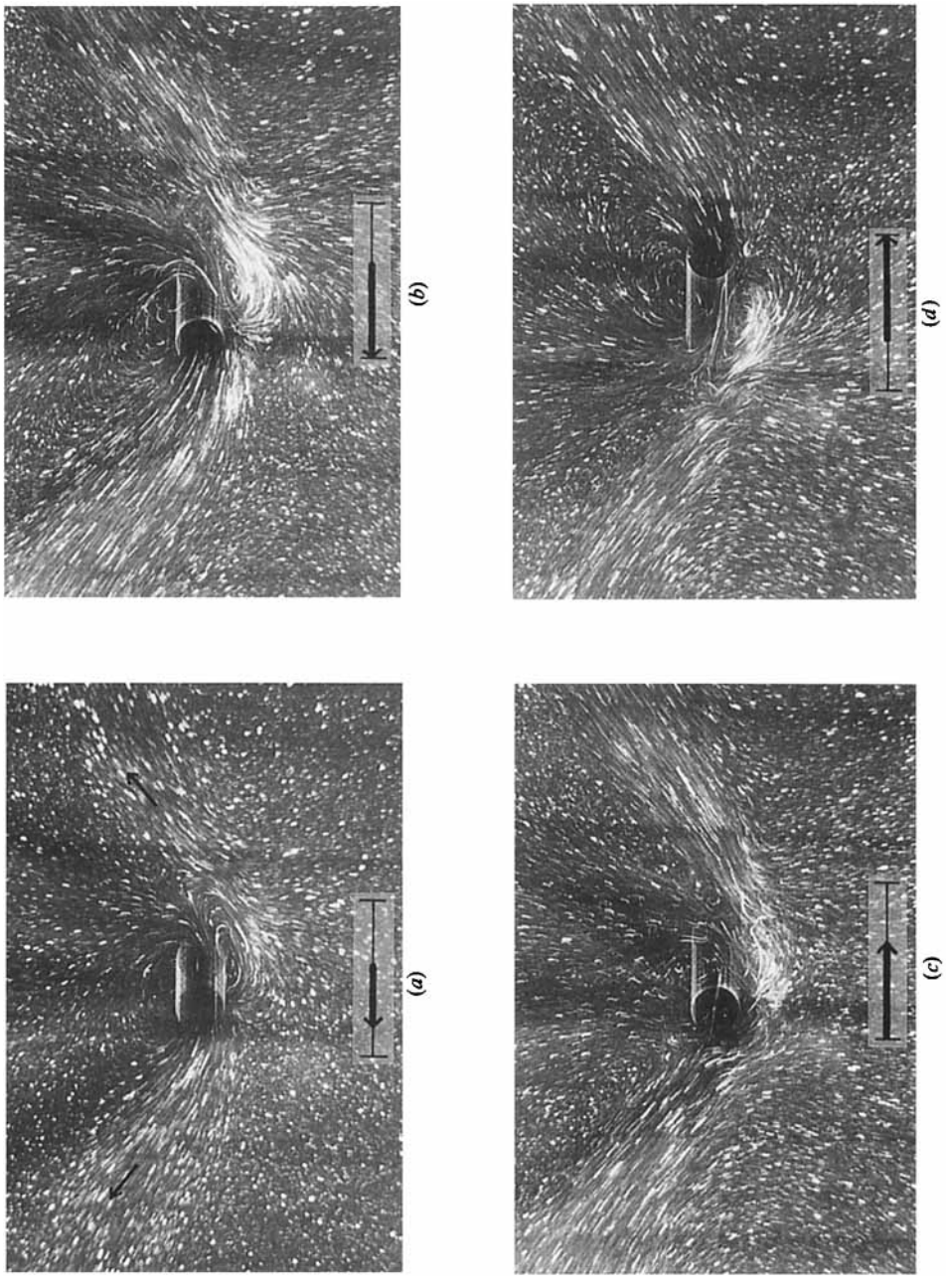

FIGURE 17. Plane views of flows in the (X, Y)-plane at various stages of motion in regime D: A1 method, $d = 1.0$ cm, $a = 1.3$ cm, $f = 0.157$ Hz, $KC = 8.16$, $\beta = 11.0$, t_e: (*a*) 1 s, (*b*)–(*d*) 2 s.

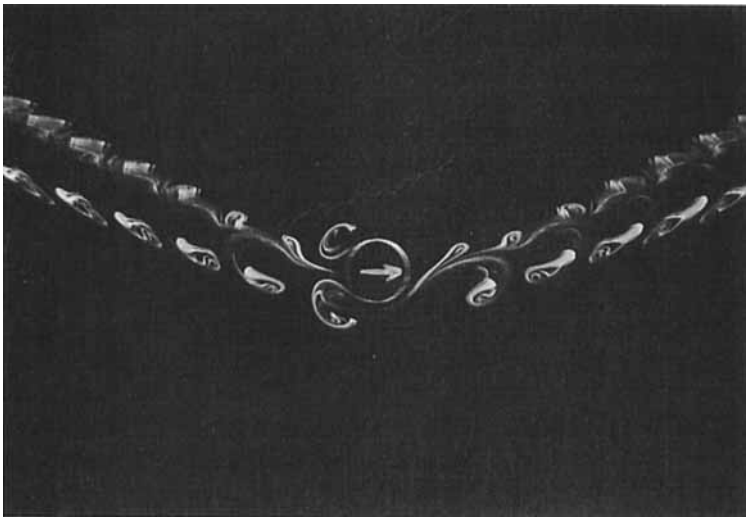

FIGURE 18. Plane view of flow in the (X, Y)-plane in regime D: e.p. method, $d = 1.0$ cm, $a = 1.0$ cm, $f = 0.246$ Hz, $KC = 6.28$, $\beta = 18.0$, $t_e = \frac{1}{16}$ s.

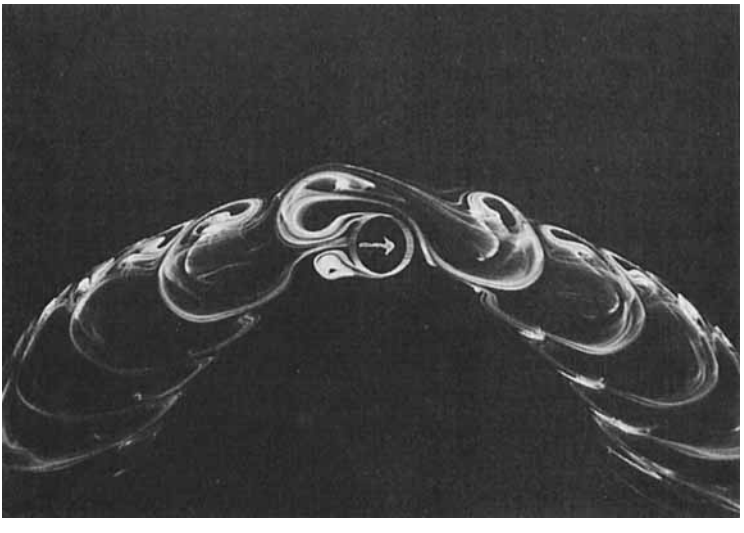

FIGURE 19. Plane view of flow in the (X, Y)-plane in regime D: e.p. method, $d = 1.0$ cm, $a = 1.0$ cm, $f = 0.303$ Hz, $KC = 6.28$, $\beta = 22.1$, $t_e = \frac{1}{16}$ s.

changes its direction to the other side. This switching of the flow occurs at irregular intervals and is presumably triggered by small disturbances. Figures 23 (*a*), 23 (*c*) and 23 (*d*) show temporarily stable flow patterns, whereas figure 23 (*b*) shows the flow changing from one side to the other.

Figure 24 shows a vertical view of the flow at an arbitrary instant in a broad section including the (X, Z)-plane. The flow has a three-dimensional structure and shows irregularity in its direction of travel up and down the cylinder and in its angle to the oscillation direction. The distance between adjacent streaked flows are variable. When the curved flow switches from one side of the cylinder to the other, the vertical streaked flow structure becomes obscure.

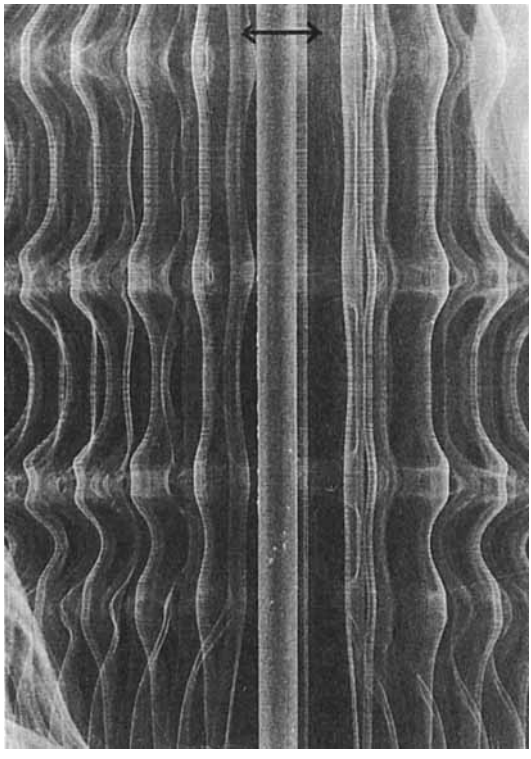

FIGURE 20. Flow pattern in a broad cross-section including the (X, Z)-plane in regime D: e.p. method, $d = 1.0$ cm, $a = 1.5$ cm, $f = 0.101$ Hz, $KC = 9.42$, $\beta = 7.83$, $t_e = \frac{1}{125}$ s.

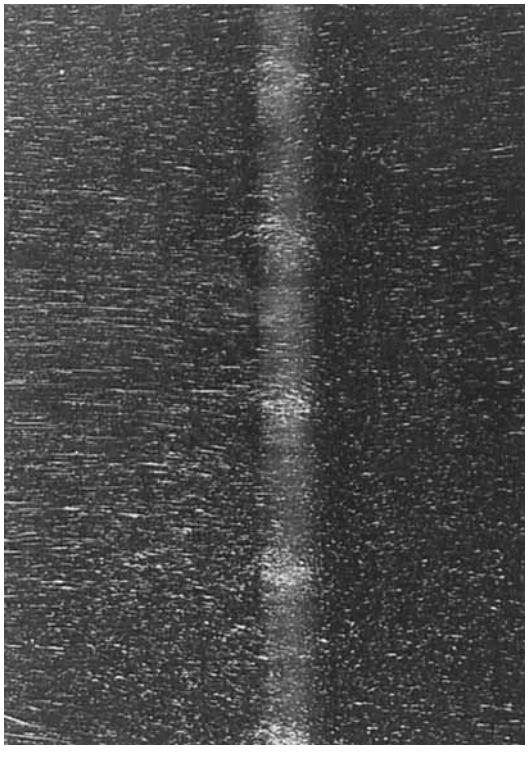

FIGURE 21. Plane view of flow in a plane perpendicular to the flow in regime D: A1 method, $d = 1.0$ cm, $a = 1.0$ cm, $f = 0.206$ Hz, $KC = 6.28$, $\beta = 22.4$, $t_e = 60$ s.

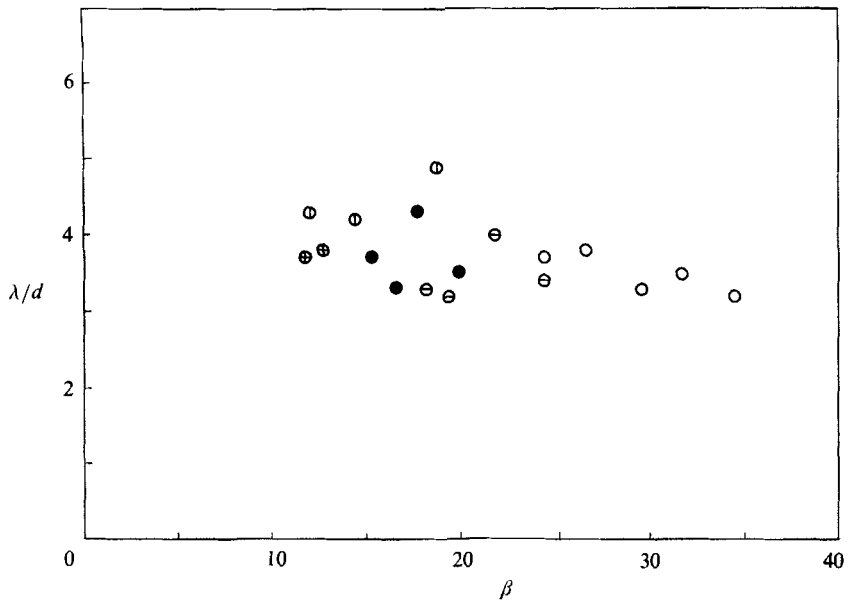

FIGURE 22. Distance between two flow tubes in regime D. ⊕, $KC = 8.16$; ⊙, 7.54; ●, 6.91; ⊖, 6.28; ○, 5.65.

3.7. *Regime* F

Figure 25 shows flow patterns in the (X, Z)-plane at various stages of the motion in regime F. When the cylinder moves from right to left, a large clockwise vortex is formed on the upper side of the cylinder and a smaller counterclockwise vortex on the lower side of the cylinder (figure 25*a*). As the clockwise vortex grows stronger a transverse flow appears behind two vortices (figure 25*b*). When the cylinder reverses, the stronger clockwise vortex is convected back to the cylinder inducing a new vortex, which is indistinct in figure 25(*c*). However it is seen clearly in figures 26(*b*) and 26(*c*). The transverse flow developed behind the cylinder distorts the trail of flow away from the oscillation axis (figure 25*c*). In the half cycle from left to right, a strong clockwise vortex and a flow crossing the axis of oscillation are developed in the same manner as in the previous half cycle (figure 25*d*).

Figure 26 shows the consecutive stages of flow development over about a half cycle, following about five cycles from the beginning of the cylinder motion. The process of the development and shedding of vortices can be seen clearly in figures 25 and 26. When the cylinder moves from right to left, a large clockwise vortex is formed (*a*). As the cylinder reverses, the strong vortex is convected back to the cylinder inducing a new vortex (*b*), and a vortex pair is formed and convects away from the cylinder (*c*).

Figure 27 shows a vertical view of the flow in the (X, Z)-plane. It will be seen that in this regime the flow also has a three-dimensional structure. Figures 28 and 29 show vertical views of the flow in the (X, Z)-plane visualized by two different methods. From these figures, it is clear that pairs of longitudinal vortices, with opposite signs of rotation, are formed at certain intervals along the axis of the cylinder.

The non-dimensional value of the distance between pairs of longitudinal vortices is plotted against β for several values of KC in figure 30. The values of λ/d are

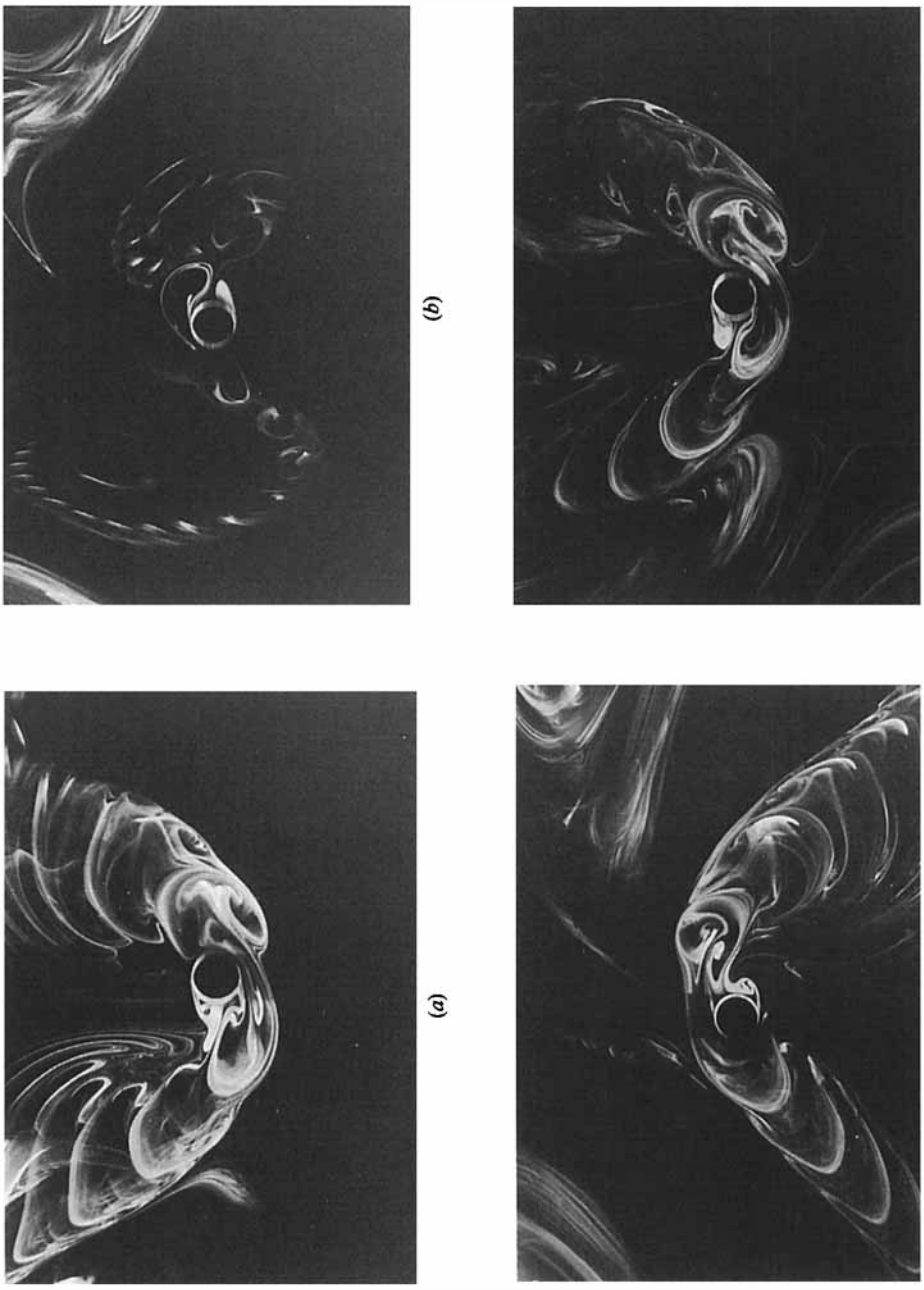

FIGURE 23. Changes of flow patterns repeated aperiodically in regime E: e.p. method, $d = 1.0$ cm, $a = 1.0$ cm, $f = 0.351$ Hz, $KC = 6.28$, $\beta = 25.6$, $t_e = \frac{1}{15}$ s.

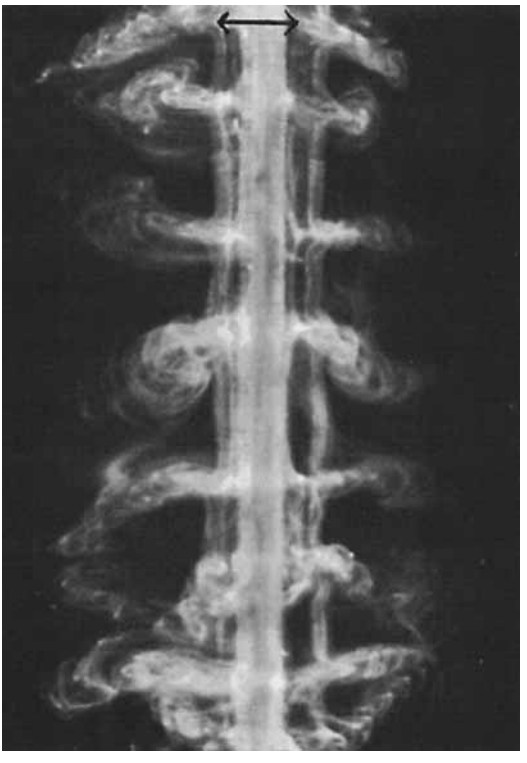

FIGURE 24. Flow pattern in a broad cross-section including the (X, Y)-plane in regime E: e.p. method, $d = 1.0$ cm, $a = 1.0$ cm, $f = 0.410$ Hz, $KC = 6.28$, $\beta = 28.7$, $t_e = \frac{1}{125}$ s.

scattered between 3.5 and 6 for $10 < \beta < 40$, and any dependence of λ/d on KC is obscure. The value of λ/d slightly decreases with increase of β and this tendency is similar to that of the flows in regime D.

Figure 31 shows an example of a flow pattern at a large KC value, in the (X, Y)-plane. It demonstrates that the path taken by the vortices deviates substantially from the direction of cylinder oscillation. The convection of vortices away from the body at large angles to the oscillation direction seems to be similar to the formation of two vortex pairs per cycle at larger β, which has been described as the '2P' pattern in Williamson (1985) and the 'diagonal' pattern by Bearman *et al.* (1981).

3.8. *Regime* G

Figure 32 shows an example of the flow in regime G. The cylinder is moving from right to left and two vortices are formed; one is attached to the cylinder and the other seems to have just been shed from the cylinder. This vortex, with a counterclockwise rotation, is shed downwards halfway through a cycle. The process of flow development is demonstrated in figure 33 in diagrammatic form. In the next half cycle from left to right, a clockwise vortex is shed downwards. As such a process is repeated, a circulatory streaming is generated around the cylinder, shown in the lower part of figure 33. This regime appears to be similar to the transverse vortex street observed by Bearman *et al.* (1981) and Williamson (1985) at higher values of β. As the values of KC or β increase, turbulent motion appears and the direction of the flow may change intermittently. The flow may have a three-dimensional structure, but this structure is not regular along the cylinder axis.

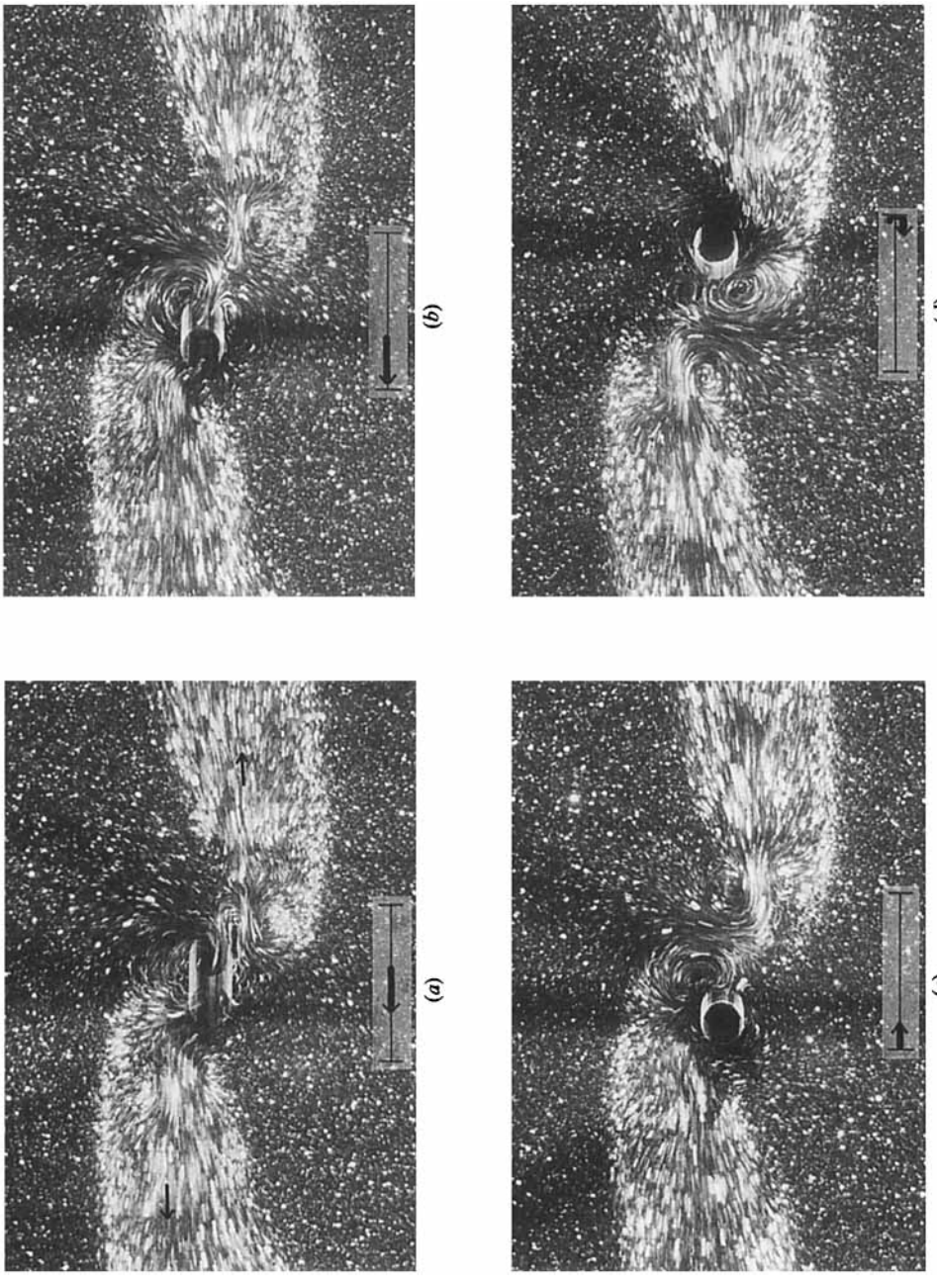

FIGURE 25. Plane view of flows in the (X, Y)-plane at various stages of motion in regime F: A1 method, $d = 1.0$ cm, $a = 1.3$ cm, $f = 0.305$ Hz, $KC = 8.16$, $\beta = 22.3$, $t_e = \frac{1}{2}$ s.

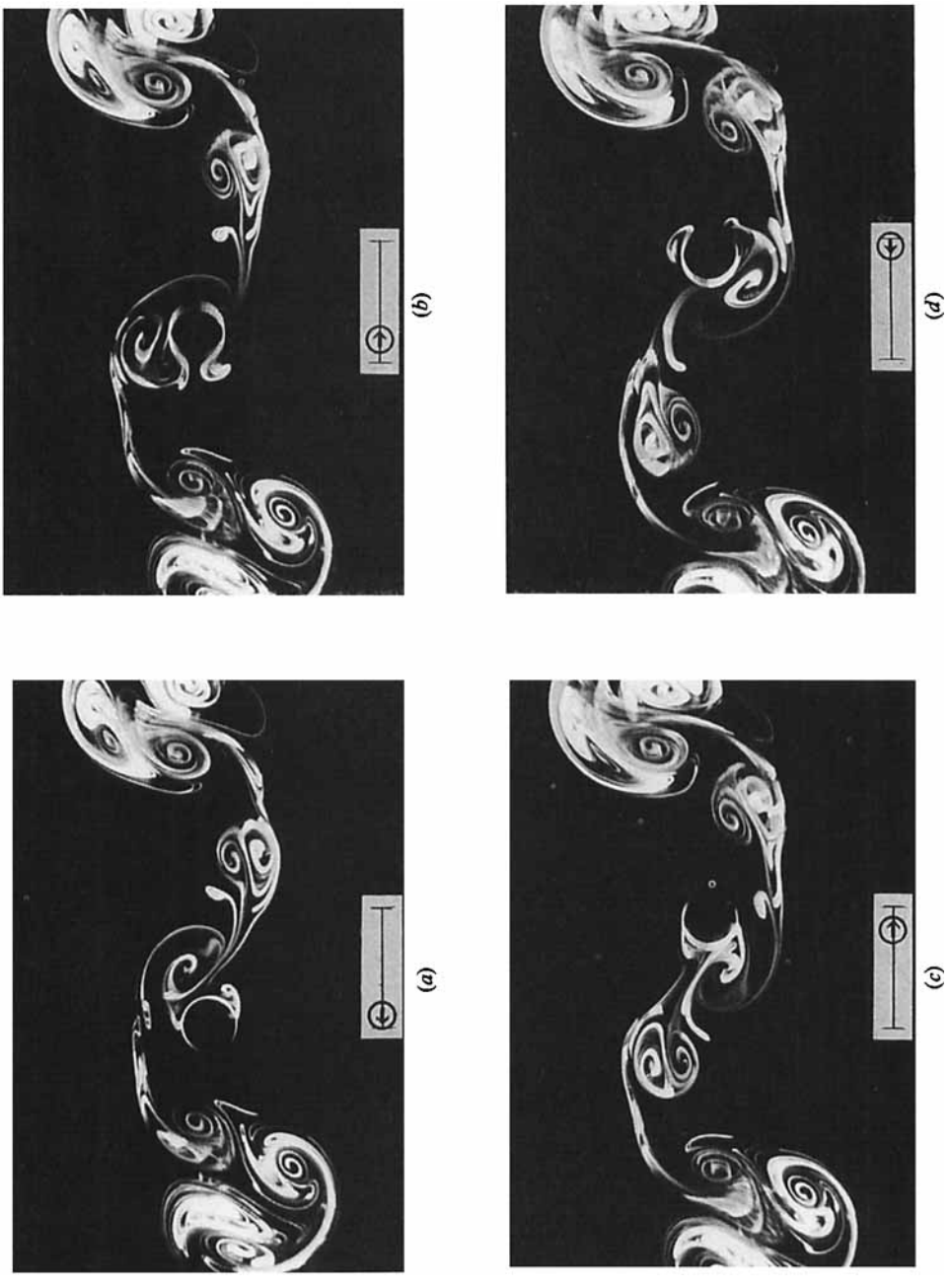

FIGURE 26. Plane view of flows in the (X, Y)-plane at consecutive stages of motion in regime F: e.p. method, $d = 1.0$ cm, $a = 1.3$ cm, $f = 0.255$ Hz, $KC = 8.16$, $\beta = 27.0$, $t_e = \frac{1}{8}$ s.

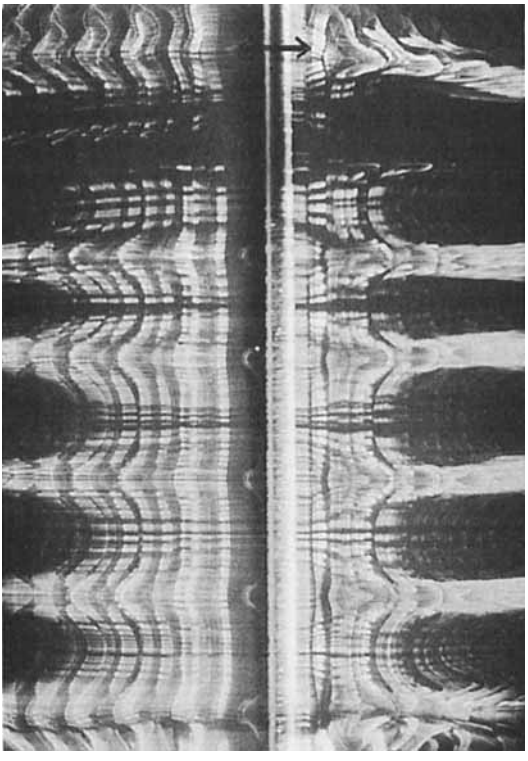

FIGURE 27. Plane view of flow in the (X, Y)-plane in regime F: e.p. method, $d = 1.0$ cm, $a = 1.5$ cm, $f = 0.164$ Hz, $KC = 9.42$, $\beta = 12.5$, $t_e = \frac{1}{15}$ s.

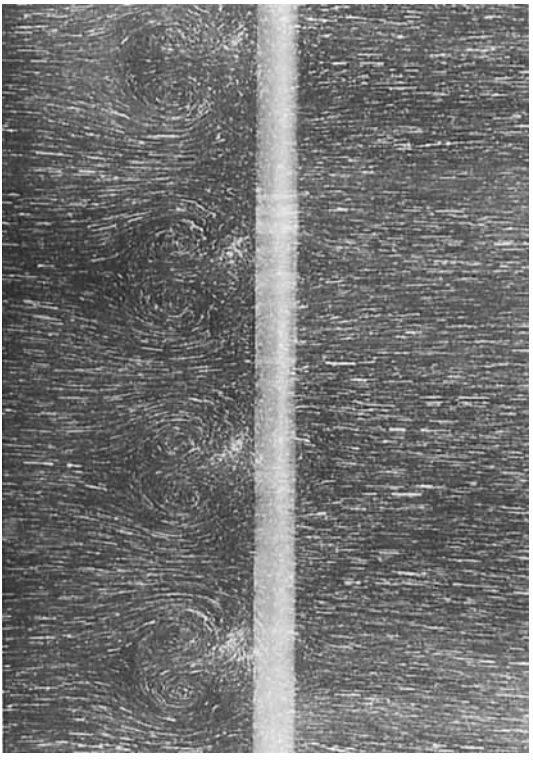

FIGURE 28. Plane view of flow in a plane at $X \doteqdot 3$ cm parallel to the (Y, Z)-plane in regime F: A1 method, $d = 1.0$ cm, $a = 1.5$ cm, $f = 0.160$ Hz, $KC = 9.42$, $\beta = 15.1$, $t_e = 15$ s.

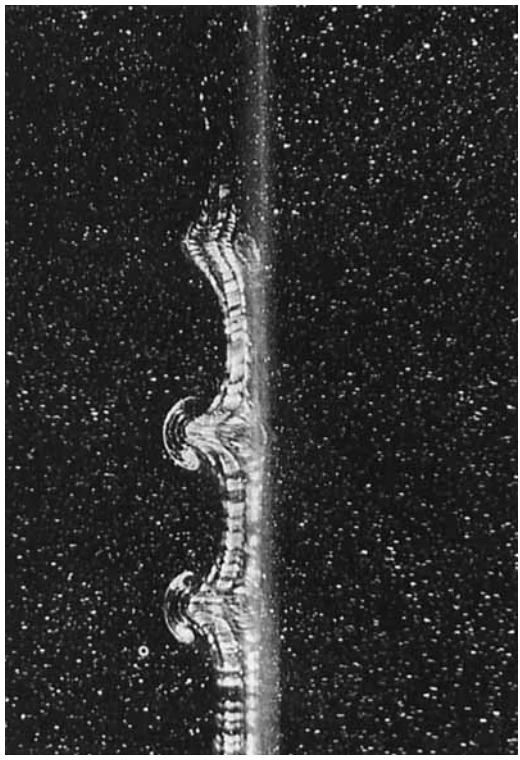

FIGURE 29. Plane view of flow in a plane at $X \doteqdot 3$ cm parallel to the (Y, Z)-plane in regime F: e.p. method, $d = 1.0$ cm, $a = 1.5$ cm, $f = 0.156$ Hz, $KC = 9.42$, $\beta = 13.8$, $t_e = 1$ s.

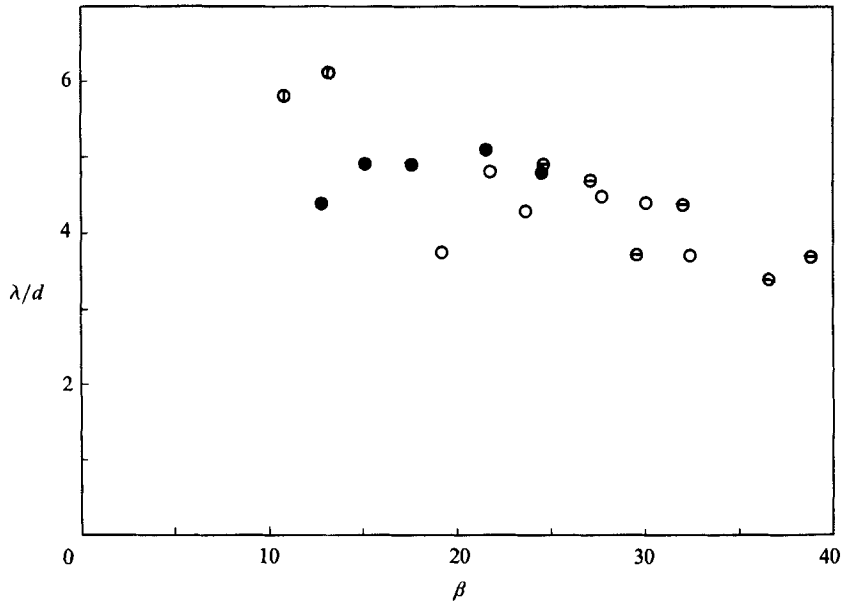

FIGURE 30. Distance between two pairs of longitudinal vortices in regime F. ○, $KC = 11.0$; ●, 9.42; ○, 8.16; ⊖, 7.54.

FIGURE 31. Plane view of flow in the (X, Y)-plane in regime F: e.p. method, $d = 1.0$ cm, $a = 2.0$ cm, $f = 0.166$ Hz, $KC = 12.6$, $\beta = 17.8$, $t_e = \frac{1}{4}$ s.

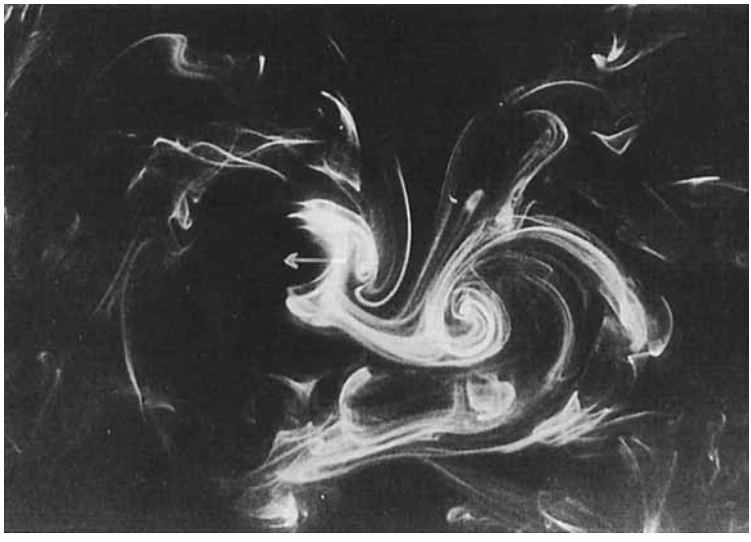

FIGURE 32. Plane view of flow in the (X, Y)-plane in regime G: e.p. method, $d = 2.0$ cm, $a = 2.63$ cm, $f = 0.10$ Hz, $KC = 8.26$, $\beta = 37.7$, $t_e = \frac{1}{15}$ s.

4. Conclusion

In this paper a circular cylinder is oscillated sinusoidally in water at rest and the structure of the resulting flow is investigated by means of flow visualization. A remarkable range of flow regimes is observed.

At small values of both KC and β, the induced flow is in line with the direction of oscillation and its structure is two-dimensional along the axis of the cylinder.

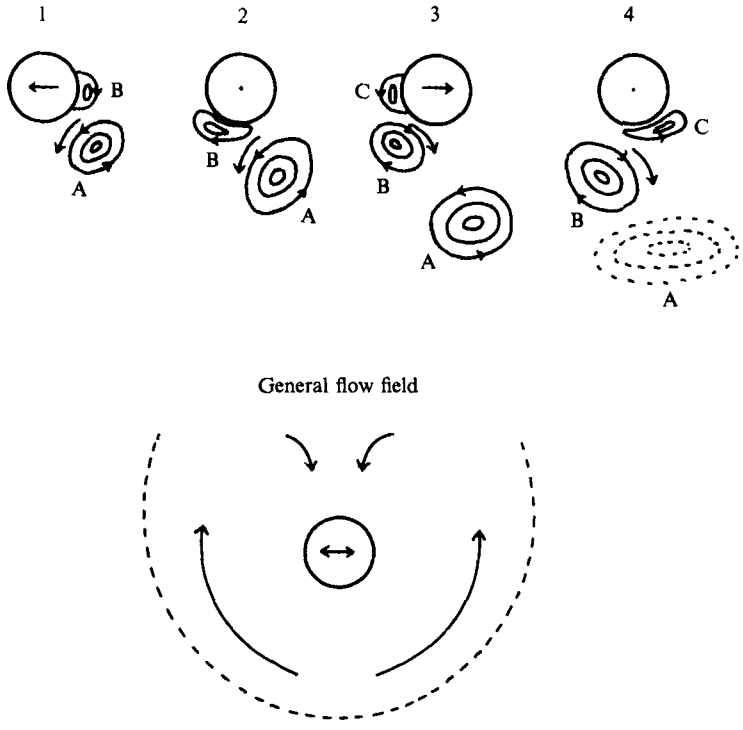

FIGURE 33. Sketch of the sequence of vortex shedding observed by means of A1 method and a general view of a circulatory streaming induced around a cylinder.

As the oscillation amplitude is increased, some asymmetry appears in the flow separation and vortex development behind the cylinder. The process of development and shedding of vortices depends on the values of KC and β, and several types of flows are generated around the cylinder. Most of the induced flows show a three-dimensional instability along the cylinder axis. The induced flow patterns are classified into eight regimes in the range $1.6 < KC < 15$ and $5 < \beta < 160$.

Regime	Principal features
A*	No flow separation; secondary streaming; two-dimensional
A	Two vortices shed symmetrically per half cycle; two-dimensional
B	Three-dimensional instability; longitudinal vortices
C	Rearrangement of large vortices; three-dimensional
D	Flow convected obliquely to one side of the axis of oscillation; three-dimensional
E	Irregular switching of flow convection direction; three-dimensional
F	Flow convected diagonally; three-dimensional
G	Transverse vortex street; three-dimensional

One of the authors (M.T.) was supported by a research fellowship from the Ministry of Education, Science and Culture of Japan. Also he would like to express his gratitude to Professor G. A. O. Davies, Head of the Department of Aeronautics at Imperial College, for his hospitality during his stay.

REFERENCES

ANDRADE, E. N. DA C. 1931 On the circulations caused by the vibration of air in a tube. *Proc. R. Soc. Lond.* A **134**, 445.

BEARMAN, P. W., DOWNIE, M. J., GRAHAM, J. M. R. & OBASAJU, E. D. 1985 Forces on cylinders in viscous oscillatory flow at low Keulegan–Carpenter numbers. *J. Fluid Mech.* **154**, 337.

BEARMAN, P. W. & GRAHAM, J. M. R. 1980 Vortex shedding from bluff bodies in oscillatory flow: A report on Euromech 119. *J. Fluid Mech.* **99**, 225.

BEARMAN, P. W., GRAHAM J. M. R., NAYLOR, P. & OBASAJU, E. D. 1981 The role of vortices in oscillatory flow about bluff cylinders. *Intl Symp. Hydrodynamics in Ocean Engineering, Norw. Inst. Tech.* 621.

HONJI, H. 1981 Streaked flow around an oscillating circular cylinder. *J. Fluid Mech.* **107**, 509.

HONJI, H., TANEDA, S. & TATSUNO, M. 1980 Some practical details of the electrolytic precipitation method of flow visualization. *Rep. Res. Inst Appl. Mech. Kyushu Univ. Japan* **28**, 83.

OBASAJU, E. D., BEARMAN, P. W. & GRAHAM, J. M. R. 1988 A study of forces, circulation and vortex patterns around a circular cylinder in oscillating flow. *J. Fluid Mech.* **196**, 467.

SARPKAYA, T. 1986 Force on a circular cylinder in viscous oscillatory flow at low Keulegan–Carpenter numbers. *J. Fluid Mech.* **165**, 61.

SCHLICHTING, H. 1932 Berechnung ebener periodischer Grenzschichtstromungen. *Z. Phys.* **33**, 327.

TANEDA, S., HONJI, H. & TATSUNO, M. 1979 *Flow visualization* (ed. T. Asanuma), p. 209. Hemisphere.

TATSUNO, M. 1973 Circulatory streaming around an oscillating Circular cylinder at low Reynolds numbers. *J. Phys. Soc. Japan* **35**, 915.

TATSUNO, M. 1981 Secondary flow induced by a circular cylinder performing unharmonic oscillations. *J. Phys. Soc. Japan* **50**, 330.

WILLIAMSON, C. H. K. 1985 Sinusoidal flow relative to circular cylinders. *J. Fluid Mech.* **155**, 141.